
Myelotoxicity and RBE of ^{211}At -Conjugated Monoclonal Antibodies Compared with $^{99\text{m}}\text{Tc}$ -Conjugated Monoclonal Antibodies and ^{60}Co Irradiation in Nude Mice

Jörgen Elgqvist, MSc¹; Peter Bernhardt, PhD¹; Ragnar Hultborn, MD, PhD²; Holger Jensen, PhD³; Börje Karlsson, PhD¹; Sture Lindegren, PhD¹; Elisabet Warnhammar²; and Lars Jacobsson, PhD¹

¹Department of Radiation Physics, The Sahlgrenska Academy at Göteborg University, Göteborg, Sweden; ²Department of Oncology, The Sahlgrenska Academy at Göteborg University, Göteborg, Sweden; and ³Positron Emission Tomography and Cyclotron Unit, Köpenhamn, Denmark

The rationale of this study was to determine the myelotoxicity in nude mice of the α -emitter ^{211}At conjugated to monoclonal antibodies (mAbs) and to compare the effect with an electron emitter, $^{99\text{m}}\text{Tc}$, and external irradiation from a ^{60}Co source, for estimation of the relative biological effectiveness (RBE). **Methods:** ^{211}At and $^{99\text{m}}\text{Tc}$ were conjugated to the IgG1 mAbs MX35 and 88BV59. Nude female BALB/c mice, 8- to 12-wk old, were injected intraperitoneally or intravenously. The biodistribution was determined 3, 6, and 18 h after injection. The bone-to-blood and bone marrow-to-blood activity concentration ratios (BBLR and BMBLR, respectively) were determined for simultaneously injected ^{211}At - and $^{99\text{m}}\text{Tc}$ -mAbs. Bone marrow samples were taken from the femur. For each mouse, the whole-body retention was measured as well as the blood activity by repeated blood samples from the tail vein (0), 1, 3, 6, 12, and 18 h after injection. External-beam irradiation from a ^{60}Co source was also performed at 3 different dose levels. White blood cell (WBC) counts, red blood cell counts, platelet counts, and hemoglobin were determined for each mouse initially and on days 1, 4, 5, 7, 15, 22, and 27 after injection. The calculations of the absorbed dose to the bone marrow were based on the BBLR, BMBLR, the cumulated activities, and the absorbed fractions. The absorbed fractions, ϕ , for α -particles and electrons in the bone marrow were calculated using Monte Carlo simulations based on a bone marrow dosimetry model. **Results:** The BMBLR was 0.58 ± 0.06 and 0.56 ± 0.06 for the ^{211}At - and $^{99\text{m}}\text{Tc}$ -mAbs, respectively. No significant variation in BMBLR with time was found. The absorbed fractions for α -particles and electrons in the bone marrow were 0.88 and 0.75, respectively. The mean absorbed fractions of the photons from $^{99\text{m}}\text{Tc}$ were 0.033 and 0.52 for 140 and 18.3 keV, respectively. When different amounts of ^{211}At - and $^{99\text{m}}\text{Tc}$ -mAbs (0.09–1.3 and 250–1,300 MBq, respectively) were administered intraperitoneally or intravenously, corresponding to absorbed doses to the bone marrow of 0.01–0.60 and 0.39–1.92 Gy, respectively, the WBC counts was

suppressed by 1%–90% and 23%–89%, respectively. When external-beam irradiation with a ^{60}Co source was performed to absorbed doses of 1.4, 1.9, and 2.4 Gy, the WBC counts was suppressed by 47%–90%. These results indicate a myelotoxic in vivo RBE of 3.4 ± 0.6 for α -particles compared with $^{99\text{m}}\text{Tc}$ and 5.0 ± 0.9 compared with ^{60}Co irradiation. **Conclusion:** The effect on the WBC counts from bone marrow irradiation with ^{211}At -mAbs indicates an in vivo RBE of 3.4 ± 0.6 in comparison with $^{99\text{m}}\text{Tc}$ -mAbs. The RBE value compared with external irradiation is 5.0 ± 0.9 .

Key Words: astatine; radioimmunotherapy; radiotoxicity; bone marrow; dosimetry

J Nucl Med 2005; 46:464–471

This study investigates the myelotoxicity and determines a value of the relative biological effectiveness (RBE) of the α -emitter ^{211}At in nude mice in comparison with an electron emitter, $^{99\text{m}}\text{Tc}$, and external irradiation. The endpoint parameter used to measure the degree of myelotoxicity in this study was white blood cell (WBC) counts. The behavior and characteristics of α -particle radiation in vivo are of fundamental radiobiologic interest, as α -particle-emitting nuclides have become increasingly more interesting as potential therapeutic agents during recent years (1–4). Coupled to monoclonal antibodies (mAbs), or fragments of antibodies, α -particle emitters provide a promising tool in treating different kinds of disseminated cancers. The investigation of possible toxic effects of potential α -radioimmunotherapies is necessary before more extensive clinical trials can be initiated. This study is restricted to myelotoxicity, as the bone marrow usually is the dose-limiting organ in radioimmunotherapy.

The most prominent characteristic of α -particles, when used for targeted therapy, is their range of only a few cell diameters, which makes them suitable for the treatment of small tumor nests or even single cells. The short range of

Received May 25, 2004; revision accepted Oct. 21, 2004.
For correspondence or reprints contact: Jörgen Elgqvist, MSc, Department of Radiation Physics, The Sahlgrenska Academy at Göteborg University, SE-413 45 Göteborg, Sweden.
E-mail: jorgen.elgqvist@radfys.gu.se

α -particles also limits the absorbed dose to normal tissue adjacent to tumors compared with many electron emitters. This is especially important when considering the irradiation of the bone marrow, where the blood stem cells are situated. To study the RBE of α -emitters in vivo, we have selected ^{211}At , one of the potential α -emitters for targeted therapy. ^{211}At decays with a half-life of 7.21 h in 2 ways: (a) via emission of an α -particle with an energy of 5.87 MeV to ^{207}Bi or (b) via electron capture to ^{211}Po . ^{207}Bi decays with a half-life of 31.55 y to ^{207}Pb (stable). ^{211}Po disintegrates with a half-life of 0.52 s to ^{207}Pb via α -particle emission of 7.45 MeV. The 5.87- and 7.45-MeV α -particles emitted in these processes have a mean linear energy transfer (LET) of 122 and 106 keV/ μm and a particle range in tissue of 48 and 70 μm , respectively. The high-LET α -particles originating from the decay of ^{211}At have a high probability of inducing irreparable damage to the DNA if they cross the cell nucleus. In vitro studies with ^{211}At -conjugated to mAbs and human serum albumin have demonstrated a RBE of 5–10 for tumor cells such as Colo-205 (5).

We recently performed 2 studies of the therapeutic effect of ^{211}At conjugated to the mAbs MX35 and MOv18 in treating experimental micrometastases of ovarian cancer in nude mice. As the results were promising, it seemed appropriate to use one of these antibodies in this study of the myelotoxic effect of α -particles. The choice of $^{99\text{m}}\text{Tc}$ (6) as the electron emitter (conversion electrons [CE]) in this study is based on its physical characteristics as well as its good accessibility through commercially available Tc/Mo-generators. $^{99\text{m}}\text{Tc}$ has a half-life of 6.01 h and an electron particle range of ~ 150 μm in tissue compared with 7.21 h and an average α -particle range of 61 μm for ^{211}At . This means that the dose rate patterns and absorbed fractions in tissue are comparable for the 2 nuclides and they are therefore suitable for estimation of the RBE in vivo for α -particles. External-beam irradiation with a ^{60}Co source was performed as a complement to obtain reference irradiation of high dosimetric accuracy.

MATERIALS AND METHODS

Radionuclides and External-Beam Irradiation

Two radionuclides, ^{211}At and $^{99\text{m}}\text{Tc}$, were used for the internal irradiation. ^{211}At was produced by the $^{209}\text{Bi}(\alpha,2n)^{211}\text{At}$ reaction in a cyclotron (Scanditronix MC32 NI; PET Center, Rigshospitalet, København, Denmark) and isolated from the irradiated targets by a dry distillation procedure described by Lindegren et al. (7). $^{99\text{m}}\text{Tc}$ was obtained from a Tc/Mo-generator (Mallinckrodt). The activity eluted in 1–2 mL was about 20–60 GBq. The injected activities of ^{211}At (0.09–1.3 MBq) and $^{99\text{m}}\text{Tc}$ (250–1,300 MBq) were measured using an ionization chamber (CRC-15R; Capintec). The external irradiation was accomplished using a ^{60}Co source (TEM Mobaltron therapy unit; Crawley, U.K.) with an activity of 18.87 TBq on March 19, 2003.

mAbs

Two mAbs were used, MX35 and 88BV59. MX35 is a murine IgG1-class mAb, developed and characterized at the Sloan-Kettering Institute, directed toward a cell-surface glycoprotein antigen of

about 95 kDa on NIH:OVCAR-3 tumor cells (8). The antigen is expressed strongly and homogeneously on 90% of human epithelial ovarian cancers (9). Dr. Kenneth Lloyd (Memorial Sloan-Kettering Cancer Center, New York) provided MX35. 88BV59 is a human IgG1-class mAb that recognizes a polypeptide complex antigen of 35–43 kDa identified in human colorectal adenocarcinoma (10) and on ovarian tumor cells. The antigen specificity of the antibodies was of no importance in this study since the mice had no tumors and the binding to normal tissue was low.

Conjugation of Antibodies

^{211}At was coupled to antibodies according to a protocol previously developed by Lindegren et al. (11). Briefly, ^{211}At (15–30 MBq) in chloroform was added to a reaction vial and the solvent was evaporated to dryness. One nanomole of *N*-succinimidyl-3-(trimethylstannyl)benzoate and 0.5 nmol of *N*-iodosuccinimide in methanol/1% acetic acid were added to give a final volume of 12 μL . After a 15-min reaction, unreacted astatine was reduced using sodium metabisulfite and the organic fraction of the labeling solvent was evaporated under a gentle stream of nitrogen. The antibody was added in 0.5 mol/L borate buffer (pH 8.5) to the crude labeling mixture and conjugation was allowed to proceed for 30 min.

The $^{99\text{m}}\text{Tc}$ conjugation was achieved using a modified SnCl conjugation method, in which $^{99\text{m}}\text{Tc}$ -sodium pertechnetate is reduced from the oxidation state of +7 to +4 and the disulfide bonds on the protein are reduced to sulfhydryl groups to allow the binding of $^{99\text{m}}\text{Tc}$ to the protein. For MX35, the phosphate-buffered saline (PBS) buffer was replaced by physiologic saline using a Sephadex G-25 PD-10 column blocked with PBS/1% bovine serum albumin (BSA) and rinsed with physiologic saline. SnCl, dissolved in reversed-osmosis water, was added to the antibody and the mixture was incubated for 45 min at 37°C, followed directly by the addition of $^{99\text{m}}\text{Tc}$ -sodium pertechnetate and further incubation for 5 min at 37°C. Finally, diethylenetriamine pentaacetic acid (DTPA) was added, dissolved in physiologic saline, to bind unreacted $^{99\text{m}}\text{Tc}$. $^{99\text{m}}\text{Tc}$ -DTPA was then separated from conjugated antibody on a Sephadex G-25 PD-10 column, blocked with PBS/1% BSA, and rinsed with physiologic saline. For 88BV59, the method began by dissolving SnCl in distilled water, which was added to the freeze-dried antibody. Thereafter, the procedure was the same as for MX35.

Animals

Nude female BALB/c *nu/nu* mice (age, 8- to 12-wk old; weight, 18.9–22.7 g) were used throughout the studies (Mollegaard & Bomholtgaard). The animals were kept at 22°C and 50–60% humidity with a light/dark cycle of 12 h. They were given standard food and water ad libitum. The animals were allowed to adapt for at least 1 wk after purchase. During the long-term and the 5-d toxicity studies, the mice were kept in separate lead-shielded cages for the first 24 h to avoid the effect of cross-irradiation between the animals from $^{99\text{m}}\text{Tc}$. With a separation of ~ 30 cm between the cages and a lead shielding of 1–2 mm between them, the cross-irradiation was considered to be negligible. After 24 h, 10 animals were kept in each cage. The Ethics Committee of Göteborg University approved all experiments.

Study Groups

Figure 1 shows an experimental flow chart indicating the times at which the different experiments in studies A, B, and C were performed.

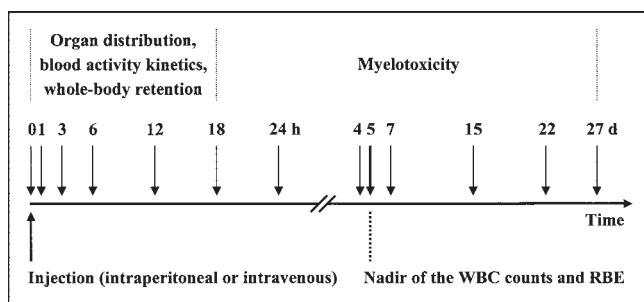


FIGURE 1. Experimental flow chart indicates times at which the different experiments in studies A, B, and C were performed.

Study A: Long-Term Study. The aim of this part of the study was to determine the temporal effect on, and the nadir of, the WBC counts. The mice were injected intraperitoneally with ~ 650 kBq ^{211}At -88BV59 ($n = 17$) or $\sim 1,200$ MBq $^{99\text{m}}\text{Tc}$ -88BV59 ($n = 30$) in 1 mL PBS. Controls animals were injected intraperitoneally with the unlabeled antibody 88BV59 ($n = 20$) in PBS or only with PBS ($n = 30$) in 1 mL. Blood samples from each animal were taken from the tail vein with thin needles to fill 10- μL heparinized hematocrit tubes before and 1, 4, 7, 15, 22, and 27 d after injection. The samples were analyzed in a microcell counter (Sysmex F-820; Toa Medical Electronics Co. Ltd.) for determination of WBC counts, red blood cell (RBC) counts, platelet (PLT) counts, and hemoglobin (HGB).

Study B: Biodistribution. In the first part of the study, the mice were injected intraperitoneally with ^{211}At -MX35 ($n = 15$), ^{211}At -88BV59 ($n = 15$), $^{99\text{m}}\text{Tc}$ -MX35 ($n = 15$), or $^{99\text{m}}\text{Tc}$ -88BV59 ($n = 15$) in 1 mL PBS. The injected amount of activity was ~ 1 MBq for the ^{211}At -mAbs and ~ 10 MBq for the $^{99\text{m}}\text{Tc}$ -mAbs. At 3, 6, and 18 h after injection the mice were sacrificed and different organs were collected: cardiac blood, lung, liver, spleen, kidney, heart, muscle (thigh), stomach, small intestine, throat (including thyroid), and bone (whole femur). In the second part of the study, the bone marrow-to-blood ratio (BMBLR) was determined by intraperitoneally coinjecting ^{211}At - and $^{99\text{m}}\text{Tc}$ -MX35 ($n = 15$) and ^{211}At - and $^{99\text{m}}\text{Tc}$ -88BV59 ($n = 15$). Samples of the bone marrow from femur and cardiac blood were taken at 3, 6, and 18 h after injection. The bone marrow of the femur was collected by isolating the femoral bone, cutting away the epiphysal ends, and introducing a thin needle to push out the contents of the diaphysal marrow cavity onto a preweighed plastic film. All samples were weighed and the activity was measured in a γ -counter (Wizard 1480; Wallace).

Study C: Five-Day Toxicity and RBE. ^{211}At - or $^{99\text{m}}\text{Tc}$ -mAbs were injected intraperitoneally or intravenously in 68 mice that were sacrificed on day 5 for determination of the WBC counts:

- Intraperitoneal injection (in 1 mL PBS): 0.09–1.3 MBq of ^{211}At -MX35 ($n = 14$) or ^{211}At -88BV59 ($n = 16$) or 250–1,300 MBq of $^{99\text{m}}\text{Tc}$ -MX35 ($n = 16$) or $^{99\text{m}}\text{Tc}$ -88BV59 ($n = 10$).
- Intravenous injection (in 0.1 mL PBS): 0.15–0.34 MBq of ^{211}At -MX35 ($n = 4$) or ^{211}At -88BV59 ($n = 4$) or 760–840 MBq of $^{99\text{m}}\text{Tc}$ -MX35 ($n = 4$).

Individual biokinetic measurements were made in most animals ($n = 58$) for calculation of the individual absorbed doses to the bone marrow from ^{211}At or $^{99\text{m}}\text{Tc}$.

The individual whole-body retention and blood activity concentration was determined at (0), 1, 3, 6, 12, and 18 h after injection.

The whole-body activity was measured with a NaI detector placed at a fixed distance from each animal. The blood samples were drawn from the tail vein to fill 10- μL heparinized hematocrit tubes. The radioactivity in the samples was measured in a γ -counter. For both the whole-body retention and the blood activity kinetics, an integration of the time-activity curve was done for each animal. This integration yielded the area under curve (AUC), which equaled the cumulated activity concentration for each animal. Numeric integration was performed from 0 to 12 h. Between 12 and 18 h, an exponential curve was fitted and integrated to infinity.

For 2 groups of animals (intraperitoneal injection of 300 MBq [$n = 5$] and 1,100 MBq [$n = 5$] of $^{99\text{m}}\text{Tc}$ -88BV59), no individual biokinetic measurements were done. Instead, mean values of the biokinetic data from study B for $^{99\text{m}}\text{Tc}$ -88BV59 were used in the absorbed dose calculation.

Regarding the integration of the blood activity curve for the intravenously injected animals, an assumption had to be made with respect to the percentage injected activity per gram (%IA/g) at time = 0. For example, if an animal weighed 19 g, a total blood volume of 1.5 mL was assumed (8%). This means that there was ~ 70 %IA/g at time = 0.

Another group of animals was externally irradiated with a ^{60}Co source ($n = 19$), giving absorbed doses of 1.4, 1.9, and 2.4 Gy. The external irradiation proceeded for 120 min for each group and was achieved by letting the animals stay in an in-house constructed cage at a fixed distance from the ^{60}Co source during the experiment. The absorbed dose from the external irradiation was verified by thermoluminescent dosimeter measurements.

For blood cell counting, samples were taken from each animal via the tail vein, before the injection or irradiation and 5 d after injection or irradiation before sacrifice, when blood also was sampled with 10- and 20- μL heparinized hematocrit tubes via direct heart puncture. The samples were analyzed in the microcell counter with regard to WBCs, RBCs, PLTs, and HGB. Reference groups, sham-injected (with PBS) or irradiated, were used as controls in these experiments. If a significant ($P < 0.05$) change in the blood cell counts (only WBC) of the control animals occurred between day 0 and day 5, the values from the irradiated animals were correspondingly adjusted. The adjustment was made in 25% of the cases and was always $< 20\%$.

Dosimetry and RBE Analysis

The mean energy deposited in various bone marrow sites of the mouse was simulated for the α -particles emitted from ^{211}At and the electrons emitted from $^{99\text{m}}\text{Tc}$. The geometries and distribution of the different bone marrow sites was simulated according to a model by Muthuswamy et al. (12): vertebra, spheres with a diameter of 0.2 mm (21% of bone marrow); skull, spheres with a diameter of 0.17 mm (12%); limb bones, cylinders with diameters of 0.9 mm and lengths of 20 mm (20%); and ribs + clavicle + sternum + pelvis, slab with a thickness of 0.3 mm (47%).

In-house Monte Carlo software was used to simulate the energy deposited in each geometry. The random generator from Matlab (Mathworks) was used to randomly locate the nuclides and choose the directions of radiation emission. The energy deposited within the marrow sites was calculated by integrating over the track length within the marrow. The scaled point kernel of Berger (13) was used for electrons, and the stopping power values from ICRU Report 49 (14) were used for the α -particles. All integration was performed by numeric summation.

To be able to calculate the absorbed dose to the bone marrow, the ratio between the activity concentrations in bone and blood as well as bone marrow and blood was defined:

$$BBLR \equiv \frac{C_{bone}}{C_{blood}}. \quad \text{Eq. 1}$$

$$BMBLR \equiv \frac{C_{bone\ marrow}}{C_{blood}}. \quad \text{Eq. 2}$$

The absorbed dose (D) to the bone marrow was then calculated by assuming a baseline cumulated activity concentration in bone marrow equal to the cumulated blood activity concentration multiplied with $BBLR$, assuming an absorbed fraction equal to 1. For the excess over baseline, the cumulated activity concentration in bone marrow was set to the cumulated blood activity concentration multiplied with $BMBLR - BBLR$. The absorbed fraction (ϕ) was in this case calculated using the Monte Carlo software for the different bone marrow geometries. Hence, the absorbed dose to the bone marrow, originating from α -particles and electrons, can be written as:

$$D = \tilde{C}_{blood} \cdot \Delta[(BMBLR - BBLR) \cdot \phi + BBLR \cdot 1], \quad \text{Eq. 3}$$

where \tilde{C}_{blood} is the cumulated blood activity concentration and Δ is the sum of the radiation energy emitted per nuclear transition.

The contribution of the photons to the absorbed dose to the bone marrow was included for ^{99m}Tc and was calculated based on the whole-body retention curves. In this case, the cumulated whole-body activity concentration was determined and the absorbed fraction of the photons was calculated by approximating the shape of the mouse to a sphere with a radius of $r = (3m/4\pi\rho_m)^{1/3}$, where m is the mass of the mouse and ρ_m is the mean tissue density. It was further assumed that both the activity and the bone marrow were homogeneously distributed throughout this sphere. The absorbed fraction was calculated as:

$$\phi(r) = 0.75 \cdot (1 - e^{-\mu_{en}r}), \quad \text{Eq. 4}$$

where μ_{en} is the energy absorption coefficient, equal to 0.027 and 0.70 cm^{-1} for the dominant photon energies 140 keV and 18.3 keV, respectively, and r is the radius of the sphere (15).

For equitoxic effects, the in vivo RBE can thus be defined as a quotient between the absorbed dose arising from electrons and photons from ^{99m}Tc and that due to α -particles from ^{211}At :

$$RBE \equiv \frac{D^{99mTc}}{D^{211At}} = \frac{\int_0^\infty C(t)_{blood}^{99mTc} dt \cdot \Delta^{99mTc(CE)} \cdot [(BMBLR^{99mTc} - BBLR^{99mTc}) \cdot \phi^{99mTc(CE)} + BBLR^{99mTc}] + \int_0^\infty C(t)_{whole\ body}^{99mTc} dt \cdot \Delta^{99mTc(\gamma)} \cdot \phi^{99mTc(\gamma)}}{\int_0^\infty C(t)_{blood}^{211At} dt \cdot \Delta^{211At(\alpha)} \cdot [(BMBLR^{211At} - BBLR^{211At}) \cdot \phi^{211At(\alpha)} + BBLR^{211At}]} \quad \text{Eq. 5}$$

where $\phi^{211At(\alpha)}$ and $\phi^{99mTc(CE)}$ is the absorbed fraction for α -particles from ^{211}At and electrons from ^{99m}Tc in the bone marrow, respectively. $\phi^{99mTc(\gamma)}$ is the absorbed fraction of the photons from ^{99m}Tc in the whole animal. $\Delta^{211At(\alpha)}$ is the sum of the radiation energy emitted per nuclear transition for α -particles from ^{211}At . $\Delta^{99mTc(CE)}$ and $\Delta^{99mTc(\gamma)}$ is the sum for the radiation emitted per nuclear transition for electrons and photons from ^{99m}Tc , respectively. The integrals represent the cumulated activity concentrations in the blood and the whole animal for ^{211}At and ^{99m}Tc , respectively. The contribution to the absorbed dose to the bone marrow from photons and electrons originating from ^{211}At was negligible.

RESULTS

Study A: Long-Term Study

The nadir of the WBC counts was reached at days 4–7 after injection for both the ^{211}At - and ^{99m}Tc -conjugated mAb 88BV59 (Fig. 2). The nadir of the WBC counts for the ^{60}Co -irradiated animals was reached at days 3–5 after irradiation (data not shown). Day 5 was chosen as a point of reference for measuring the myelotoxicity. The WBC counts seemed to be completely recovered 14 d after injection. No difference in recovery time was observed between ^{211}At -, ^{99m}Tc -88BV59, or ^{60}Co -irradiated animals. The variations in WBCs, RBCs, PLTs, and HGB (Fig. 2) during the observation time for the control groups were insignificant, and the mean values \pm SEM were $5.7 \pm 0.3 (\times 10^9/\text{L})$, $6.7 \pm 0.4 (\times 10^{12}/\text{L})$, $681 \pm 29 (\times 10^9/\text{L})$ and $130 \pm 4.9 (\text{g/L})$, respectively.

Study B: Biodistribution

The organ-to-blood ratios for the various combinations of radioimmunocomplexes did not differ dramatically (Table 1). For ^{99m}Tc -88BV59, an elevated organ-to-blood ratio of 1.9 ± 0.24 was found 6 h after injection in the kidneys. For ^{211}At -88BV59, a ratio of 8.93 ± 1.56 was found in the thyroid 18 h after injection. When investigating the BMBLR at 3, 6, and 18 h after injection, we observed no significant variation with time for any of the radioimmunocomplexes. The difference between the various combinations of radionuclide and mAb was small. The mean value of the BMBLR (at 3, 6, and 18 h) for ^{211}At -mAbs (MX35 and 88BV59) and ^{99m}Tc -mAbs (MX35

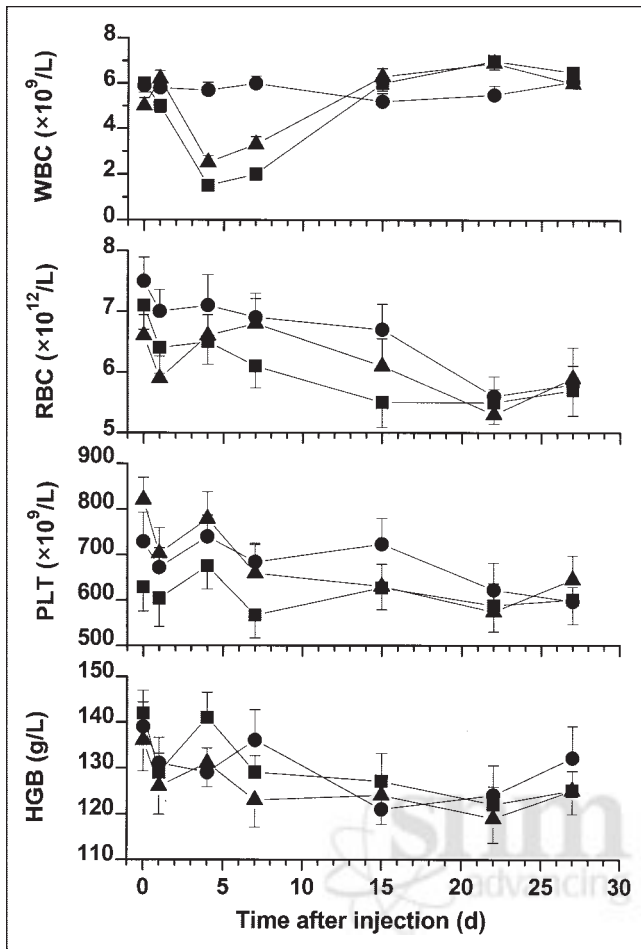


FIGURE 2. WBC counts, RBC counts, PLT counts, and HGB as function of time after injection during the long-term study, when animals were injected intraperitoneally with ^{211}At -conjugated (\blacktriangle) and $^{99\text{m}}\text{Tc}$ -conjugated (\blacksquare) mAb 88BV59 ($n = 17$ and 30 , respectively), giving an absorbed dose to bone marrow of approximately 0.3 and 1.3 Gy, respectively. The nadir of WBC counts was reached at days 4 – 7 . Results from control animals (unlabeled antibody 88BV59 [$n = 20$] and PBS [$n = 30$]) are also plotted (\bullet). Since no significant ($P > 0.05$) difference between unlabeled antibody and PBS was observed, the 2 control groups were put together. Day 5 was chosen as the reference point when comparing myelotoxicity of different combinations of nuclide and antibody (Fig. 5). Values are means \pm SEM.

and 88BV59) was 0.58 ± 0.06 and 0.56 ± 0.06 , respectively (Table 1). The weight of the bone marrow samples varied between 4 and 10 mg.

Study C: Five-Day Toxicity and RBE

The whole-body retention curves decline exponentially with a final biologic half-life of ~ 18 h for both the ^{211}At - and $^{99\text{m}}\text{Tc}$ -mAbs (MX35 and 88BV59) (Fig. 3). The curves in Figure 3 also include animals injected intravenously, as no variation was seen on the whole-body retention for these animals compared with those injected intraperitoneally.

For the intraperitoneally injected radioimmunocomplexes, the maximum activity concentration in the blood varied between 14 %IA/g and 21 %IA/g 3 h after injection

TABLE 1
Organ-to-Blood Ratios, Including BBLR and BMBLR, for ^{211}At - and $^{99\text{m}}\text{Tc}$ -Conjugated mAbs MX35 and 88BV59 ($n = 90$)

	3 h			6 h			18 h		
	MX35		88BV59	MX35		88BV59	MX35		88BV59
	^{211}At	$^{99\text{m}}\text{Tc}$	^{211}At	$^{99\text{m}}\text{Tc}$	^{211}At	$^{99\text{m}}\text{Tc}$	^{211}At	$^{99\text{m}}\text{Tc}$	
Blood (cardiac)	1	1	1	1	1	1	1	1	
Bone (BBLR)	0.18 \pm 0.04	0.13 \pm 0.05	0.35 \pm 0.07	0.16 \pm 0.09	0.45 \pm 0.07	0.16 \pm 0.04	0.22 \pm 0.05	0.11 \pm 0.09	0.46 \pm 0.09
Bone marrow (BMBLR)	0.54 \pm 0.12	0.54 \pm 0.10	0.58 \pm 0.10	0.61 \pm 0.10	0.61 \pm 0.12	0.58 \pm 0.10	0.59 \pm 0.12*	0.58 \pm 0.10*	0.56 \pm 0.10*
Heart	0.26 \pm 0.05	0.35 \pm 0.09	0.41 \pm 0.07	0.46 \pm 0.09	0.48 \pm 0.09	0.50 \pm 0.10	0.34 \pm 0.07	0.43 \pm 0.09	0.45 \pm 0.09
Kidney	0.27 \pm 0.05	0.92 \pm 0.12	0.46 \pm 0.10	1.10 \pm 0.14	0.62 \pm 0.12	1.90 \pm 0.24	0.31 \pm 0.05	1.06 \pm 0.12	0.58 \pm 0.10
Liver	0.30 \pm 0.05	0.31 \pm 0.07	0.26 \pm 0.05	0.40 \pm 0.09	0.37 \pm 0.05	0.54 \pm 0.09	0.33 \pm 0.07	0.37 \pm 0.09	0.49 \pm 0.09
Lung	0.48 \pm 0.07	0.54 \pm 0.12	0.66 \pm 0.10	0.34 \pm 0.09	0.62 \pm 0.14	0.79 \pm 0.16	0.49 \pm 0.09	0.58 \pm 0.12	0.73 \pm 0.16
Muscle	0.09 \pm 0.02	0.11 \pm 0.04	0.09 \pm 0.02	0.14 \pm 0.04	0.13 \pm 0.02	0.13 \pm 0.02	0.11 \pm 0.02	0.14 \pm 0.04	0.12 \pm 0.04
Small intestine	0.11 \pm 0.04	0.29 \pm 0.05	0.36 \pm 0.07	0.42 \pm 0.09	0.45 \pm 0.09	0.49 \pm 0.07	0.15 \pm 0.04	0.41 \pm 0.07	0.42 \pm 0.07
Spleen	0.33 \pm 0.07	0.49 \pm 0.09	0.38 \pm 0.07	0.50 \pm 0.09	0.49 \pm 0.10	0.62 \pm 0.12	0.48 \pm 0.09	0.51 \pm 0.10	0.47 \pm 0.07
Stomach	0.22 \pm 0.04	0.45 \pm 0.05	0.66 \pm 0.12	0.52 \pm 0.05	0.32 \pm 0.09	0.81 \pm 0.14	0.34 \pm 0.07	0.50 \pm 0.05	0.71 \pm 0.14
Thyroid†	4.19 \pm 0.89	1.76 \pm 0.36	6.34 \pm 1.15	2.01 \pm 0.46	8.70 \pm 1.48	1.82 \pm 0.39	6.48 \pm 1.24	1.99 \pm 0.38	8.93 \pm 1.56

*Extrapolated from ^{125}I measurements.

†Activity concentration (ec) in thyroid was calculated considering weight (w) of and activity (a) in throat specimen and a standard weight (sw) of thyroid of 3 mg for nude BALB/c nu/nu mice. Throat was assumed to contain samples of both muscle and thyroid. Calculation was done as follows: Thyroid_{ac} = (Throat_a - Thyroid_{sw}) \times Muscle_{ac}/Thyroid_{sw}. Values are means \pm SEM.

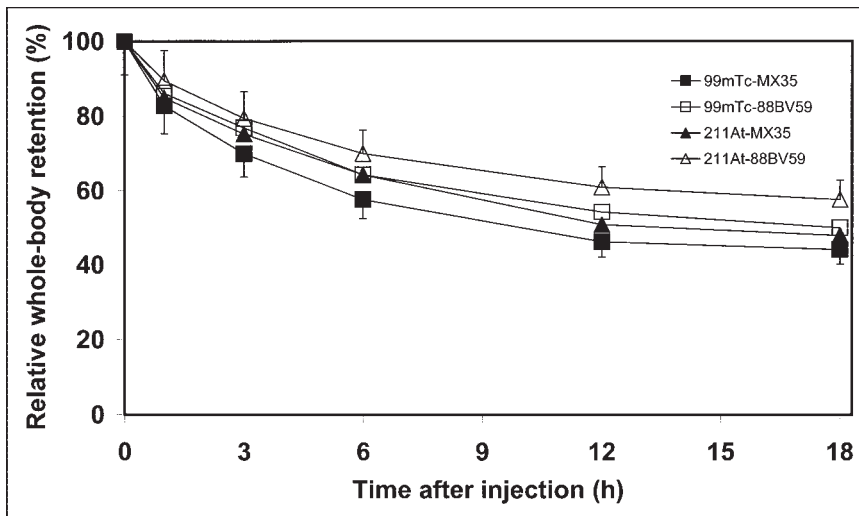


FIGURE 3. Whole-body retention for intraperitoneally (i.p.) or intravenously (i.v.) injected ^{211}At -MX35 (\blacktriangle , $n = 14$ [i.p.] and $n = 4$ [i.v.]), ^{211}At -88BV59 (\triangle , $n = 16$ [i.p.] and $n = 4$ [i.v.]), $^{99\text{m}}\text{Tc}$ -MX35 (\blacksquare , $n = 16$ [i.p.] and $n = 4$ [i.v.]), and $^{99\text{m}}\text{Tc}$ -88BV59 (\square , $n = 10$ [i.p.]) at 0, 1, 3, 6, 12, and 18 h after injection. Whole-body retention curves were used to estimate cumulated activity (i.e., AUC) and, hence, the photon contribution to absorbed dose from $^{99\text{m}}\text{Tc}$ for each individual animal. Values are means \pm SEM.

(Fig. 4). For the intravenous injections, a value of 42–56 %IA/g was observed after 1 h.

The absorbed fractions (ϕ) for α -particles and electrons in the bone marrow were calculated to 0.88 and 0.75, respectively. The absorbed fraction of the photons from $^{99\text{m}}\text{Tc}$ was calculated to 0.033 for 140 keV and 0.52 for 18.3 keV.

For the ^{211}At -mAbs (MX35 and 88BV59), the absorbed doses to the bone marrow varied between 0.01 and 0.60 Gy, causing a suppression of the WBC counts of 1%–90%. For the $^{99\text{m}}\text{Tc}$ -mAbs, the absorbed doses to the bone marrow varied between 0.39 and 1.92 Gy, causing a suppression of the WBC counts of 23%–89%. Two animals that received 2 Gy to the bone marrow from irradiation of $^{99\text{m}}\text{Tc}$ did not survive until day 5. In Figure 5, individual suppression in WBC counts is given as a function of the individually calculated absorbed doses to the bone marrow. The data points for 2 groups ($n = 10$ each) with no individual absorbed doses are shown as mean WBC count suppression and mean absorbed dose.

For the externally irradiated animals, the absorbed dose to the bone marrow was 1.4, 1.9, and 2.4 Gy, causing a

suppression of the WBC counts of 47%–90% (Fig. 5). Exponential fits were made to the ^{211}At , $^{99\text{m}}\text{Tc}$, and external irradiation data and are shown in Figure 5 (together with the 95% confidence intervals).

The in vivo RBE for myelotoxicity for the suppression of WBC counts for the α -particles from ^{211}At , calculated from the equations describing the exponential fits in Figure 5, was determined to be 3.4 ± 0.6 in relation to the electrons from $^{99\text{m}}\text{Tc}$ and 5.0 ± 0.9 in relation to external irradiation using ^{60}Co .

DISCUSSION

Since the bone marrow in general is a dose-limiting and critical organ, it is of utmost importance to elucidate any toxic effects during radioimmunotherapy; this is true for both α -particles and electrons. The myelotoxic effect of electron emitters is rather well known by several clinical trials using ^{131}I - and ^{90}Y -labeled mAbs. For α -emitters, which recently were proposed for treatment of especially micrometastases, the clinical experience for the present is very limited.

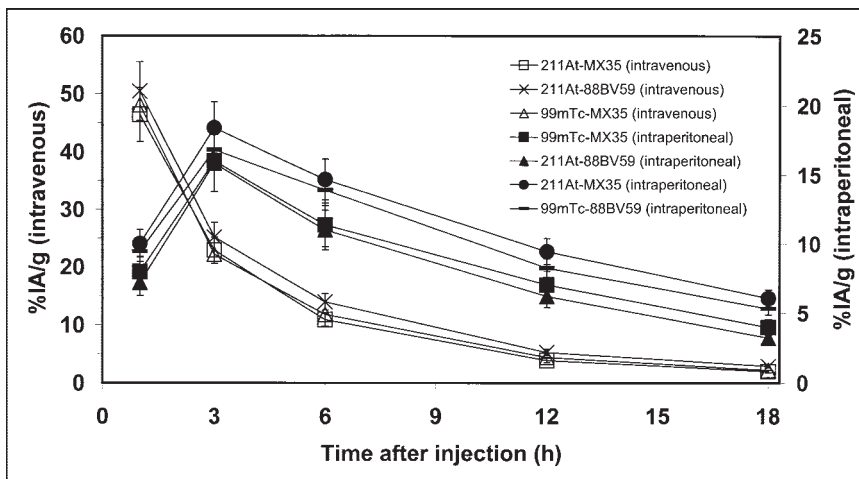


FIGURE 4. Blood activity kinetics for intraperitoneally injected ^{211}At -MX35 (\blacksquare , $n = 14$), ^{211}At -88BV59 (\blacktriangle , $n = 16$), $^{99\text{m}}\text{Tc}$ -MX35 (\blacksquare , $n = 16$), and $^{99\text{m}}\text{Tc}$ -88BV59 (\square , $n = 10$) as well as for intravenously injected ^{211}At -MX35 (\square , $n = 4$), ^{211}At -88BV59 (\times , $n = 4$), and $^{99\text{m}}\text{Tc}$ -MX35 (\triangle , $n = 4$) at 1, 3, 6, 12, and 18 h after injection. Individual curves for each animal were used to estimate cumulated activity (i.e., AUC) and, hence, the contribution from α -particles or electrons, originating from decays of ^{211}At and $^{99\text{m}}\text{Tc}$, respectively, to absorbed dose to bone marrow for each individual animal. Values are means \pm SEM.

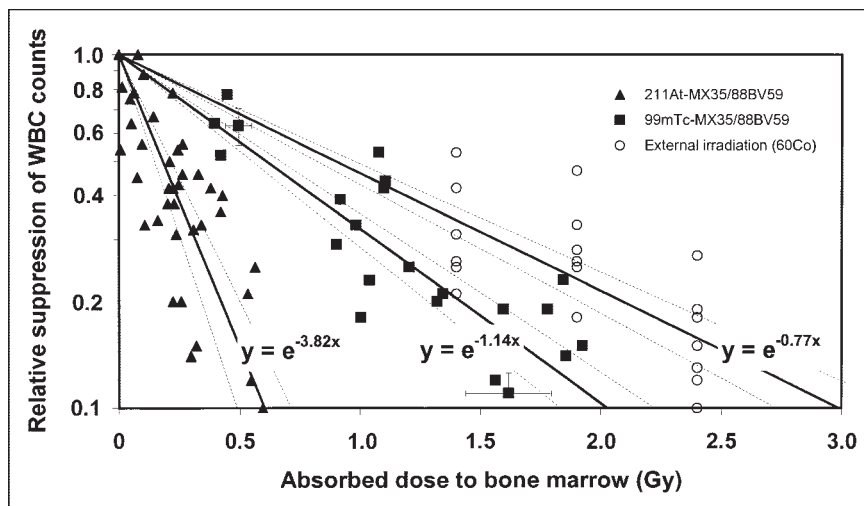


FIGURE 5. Relative suppression of WBC counts as function of absorbed dose to bone marrow in nude mice when injected with ^{211}At -conjugated (\blacktriangle , $n = 38$) and $^{99\text{m}}\text{Tc}$ -conjugated (\blacksquare , $n = 20$) mAbs or when irradiated externally with a ^{60}Co source (\circ , $n = 19$). The y-axis is logarithmic, where 1 represents no suppression and 0.1 represents 90% suppression of WBC counts. Solid lines represent exponential fits to ^{211}At and $^{99\text{m}}\text{Tc}$ data. Dashed lines flanking each full line represent 95% confidence interval. In vivo RBE

is defined as quotient of absorbed dose from $^{99\text{m}}\text{Tc}$ and that from ^{211}At for equal toxic effect—that is, for equal degrees of suppression of WBC counts. The 2 data points with error bars originate from preliminary experiments with $^{99\text{m}}\text{Tc}$ -88BV59, where cumulated blood activity concentrations and suppression of WBC counts were investigated in separate animals (\blacksquare , $n = 10$).

Recently, we performed experimental therapeutic studies using the α -particle emitter ^{211}At coupled to the mAb MOv18 (2). After intraperitoneal injection of about 0.5 MBq, good therapeutic results were obtained in nude mice with microscopic intraperitoneal growth of ovarian cancer. The median survival for treated mice was 213 d compared with 138 d for untreated mice. Thirty-three percent of the mice were apparently free of cancer after 7 mo and were probably cured. No undesirable side effects were observed, although we did not record the WBC counts. The follow-up time was up to 7 mo.

There are only a few reports on RBE in vivo regarding α -particle emitters. In one study in mice, the α -particle emitter ^{213}Bi and the electron emitter ^{90}Y were compared, and an argument was made for a RBE of 1.0 (16). An objection that can be raised to that study is that the half-life of ^{213}Bi is 45.6 min and that of ^{90}Y is 64 h, implying a considerable difference in the dose rate pattern between the 2 isotopes, making estimation of the RBE uncertain. Also, the particle ranges differ between the α -particles from ^{213}Bi and the electrons from ^{90}Y , making the absorbed dose distribution unequal for the 2 isotopes. There is not a wealth of literature with regard to the nadir of WBCs in animals injected with ^{211}At . One study from 1952 reported “the accumulation, metabolism, and biological effects of astatine in rats and monkeys” (17). In that study, a leukopenic nadir at day 5 was recognized.

The distribution in bone marrow of the radionuclide may depend on the molecule size of the labeled product and the amount of free radionuclide. Obviously, the radiochemical purity of the injected substance is of importance in a study of myelotoxicity. In all of our experiments, the ^{211}At - and $^{99\text{m}}\text{Tc}$ -conjugated mAbs were efficiently separated from free astatine or technetium using the Sephadex G-25 PD-10 column after conjugation, immediately before beginning the experiments, implying high radiochemical purity at the time of injection. The in vivo stability of the complexes was not specifically

studied. However, as no appreciable high radionuclide uptake was found in tissues that are known to enrich free radionuclides—for example, the thyroid and stomach—the ^{211}At - and $^{99\text{m}}\text{Tc}$ -radioimmunocomplexes seem to be stable in vivo during the duration of these studies—that is, up to 18 h.

Regarding the BMBLR, a value of about 0.57 was found for both the ^{211}At - and $^{99\text{m}}\text{Tc}$ -conjugated mAbs. This is expected for stable radionuclide-antibody complexes when the BMBLR reflects the distribution of the antibodies in the bone marrow. The 0.57 value, however, is somewhat higher than that found in the literature. The absorbed dose calculation is critically determined by BMBLR. However, in the determination of RBE in relation to $^{99\text{m}}\text{Tc}$ -mAbs, variations in BMBLR will partially cancel (Eq. 5).

The blood activity kinetics was determined individually to eliminate errors caused by the injection. Considerable differences in the blood activity were sometimes observed between the animals after intraperitoneal injections. This difference may be explained by the location of the injection. If the solution is injected intraintraintestinally or into a pocket between the viscera, transport of the activity into and throughout the peritoneum could be hindered, resulting in delayed diffusion into the blood circulation.

For accurate calculations of the absorbed fractions in bone marrow for the α -particles and electrons, one has to know the exact dimensions and the correct distribution of active bone marrow in mice, as well as the distribution of the radioimmunocomplexes on a microscopic level in this bone marrow. An accurate detailed geometric model of the bone marrow on the microscopic level is thus desirable. However, the model used in this work may be acceptable for the purpose of comparing the effect of ^{211}At and $^{99\text{m}}\text{Tc}$. As the radionuclides have comparable particle ranges, an error in the geometry will affect the absorbed fraction in a similar way for ^{211}At and $^{99\text{m}}\text{Tc}$. In the RBE calculation for ^{211}At , where $^{99\text{m}}\text{Tc}$ is used as a reference,

the absorbed fractions of the 2 radionuclides appear essentially as a ratio, implying that geometry errors are partially eliminated in the RBE determination (Eq. 5).

However, it cannot be ruled out that the absorbed dose to different blood stem cells could differ from the calculated mean absorbed dose to the bone marrow. The blood stem cells could, for example, be situated close to compact bone or fat cells, which could hinder some radioimmunocomplexes to reach them. This effect is also quite obvious for the very short-range ($\approx 0.2 \mu\text{m}$) electrons from $^{99\text{m}}\text{Tc}$. They constitute 13% of the emitted electron energy and 8% of the mean absorbed dose but do probably not contribute to the absorbed dose to the cell nucleus and the myelotoxicity. The only possible way those electrons could contribute to the myelotoxicity is if they were internalized into the blood stem cells to reach the DNA in the cell nucleus. However, if this does not happen, the RBE should consequently be reduced by 8% and, hence, be 3.1 instead.

The photon contribution is not negligible with regard to the irradiation from $^{99\text{m}}\text{Tc}$. It constitutes approximately 45% for intraperitoneal and 37% for intravenous injection of the bone marrow dose from $^{99\text{m}}\text{Tc}$. The 140- and 18.3-keV photons contribute to 92% and 8% of the total photon contribution from $^{99\text{m}}\text{Tc}$, respectively. The overall photon contribution could be somewhat overestimated as the animals were approximated as spheres. On the other hand, the irradiation of the bone marrow from activity in the abdomen for intraperitoneal injections could be underestimated because of the large bone marrow content in the pelvic region. There is, however, no tendency in the WBC count results indicating a discrepancy in the calculated absorbed doses for the 2 injection routes. The photon and electron contribution from the decay of ^{211}At is negligible and was not considered in the calculations of the absorbed doses.

External-beam irradiation with the ^{60}Co source was performed to provide reference irradiation with high accuracy in the absorbed dose to the bone marrow from electrons (approximately homogeneous absorbed dose in the whole mouse). The discrepancy seen in Figure 5 between the effect of this external irradiation and the effect of $^{99\text{m}}\text{Tc}$ may, aside from the uncertainty in absorbed dose calculation discussed here, be due to 2 factors: an effect of different dose rate patterns between the 2 irradiation modalities and a difference in absorbed dose to the different mice organs. The long irradiation time with declining dose rate for $^{99\text{m}}\text{Tc}$ could not be fully simulated with ^{60}Co irradiation, which may have biologic implications. The absorbed dose distribution from the external irradiation is almost homogeneous, whereas the internal radiation gives different organ doses.

CONCLUSION

The effect on the WBC counts of bone marrow irradiation with ^{211}At -mAbs indicates an in vivo RBE of 3.4 ± 0.6 in comparison with $^{99\text{m}}\text{Tc}$ -mAbs. The RBE value compared with external irradiation is 5.0 ± 0.9 . The discrepancy between the

2 RBE values may be explained by errors in the internal dosimetry for $^{99\text{m}}\text{Tc}$ or may be an effect of the difference in dose rate patterns between the $^{99\text{m}}\text{Tc}$ -mAb irradiation and the external ^{60}Co irradiation. The RBE value based on the comparison with $^{99\text{m}}\text{Tc}$ -mAbs may be the most accurate as errors in the internal dosimetry for the 2 radionuclides are partially canceled and the dose rate patterns are nearly the same.

ACKNOWLEDGMENTS

This work was supported by grants from the Swedish Cancer Foundation (3548) and the King Gustaf V Jubilee Clinic Research Foundation in Göteborg, Sweden. Special thanks go to Kenneth Lloyd at the Memorial Sloan-Kettering Cancer Center for making mAb MX35 accessible for this study.

REFERENCES

1. Andersson H, Lindegren S, Bäck T, et al. Radioimmunotherapy of nude mice with intraperitoneally growing ovarian cancer xenograft utilizing ^{211}At -labelled monoclonal antibody MOv18. *Anticancer Res.* 2000;20:459–462.
2. Andersson H, Lindegren S, Bäck T, et al. The curative and palliative potential of the monoclonal antibody MOv18 labelled with ^{211}At in nude mice with intraperitoneally growing ovarian cancer xenografts: a long term study. *Acta Oncol.* 2000;39:741–745.
3. Jurcic JG, Larson SM, Sgouros G, et al. Targeted α particle immunotherapy for myeloid leukemia. *Blood.* 2002;100:1233–1239.
4. Andersson H, Elmqvist J, Horvath G, et al. Astatine-211-labeled antibodies for treatment of disseminated ovarian cancer: an overview of results in an ovarian tumor model. *Clin Cancer Res.* 2003;9:3914–3921.
5. Palm S, Andersson H, Bäck T, et al. In vitro effects of free ^{211}At , ^{211}At -albumin and ^{211}At -monoclonal antibody compared to external photon irradiation on two human cancer cell lines. *Anticancer Res.* 2000;20:1005–1012.
6. Narra VR, Sastry KS, Goddu SM, Howell RW, Strand SE, Rao DV. Relative biological effectiveness of $^{99\text{m}}\text{Tc}$ radiopharmaceuticals. *Med Phys.* 1994;21:1921–1926.
7. Lindegren S, Bäck T, Jensen HJ. Dry-distillation of [^{211}At]-astatine from irradiated bismuth targets: a time-saving procedure with high recovery yields. *Appl Radiat Isot.* 2001;55:157–160.
8. Welshinger M, Yin BWT, Lloyd KO. Initial immunochemical characterization of MX35 ovarian cancer antigen. *Gyn Oncol.* 1997;67:188–192.
9. Rubin SC, Kostakoglu L, Divgi C, et al. Biodistribution and intraoperative evaluation of radiolabeled monoclonal antibody MX35 in patients with epithelial ovarian cancer. *Gyn Oncol.* 1993;51:61–66.
10. Serafini AN, Klein JL, Wolf BG, et al. Radioimmunoscintigraphy of recurrent, metastatic, or occult colorectal cancer with technetium $^{99\text{m}}$ -labeled totally human monoclonal antibody 88BV59: results of pivotal, phase III multicenter studies [published correction appears in *J Clin Oncol.* 1998;16:2575]. *J Clin Oncol.* 1998;16:1777–1787.
11. Lindegren S, Andersson H, Bäck T, Jacobsson L, Karlsson B, Skarnemark G. High-efficiency astatination of antibodies using *N*-iodosuccinimide as the oxidising agent in labelling *N*-succinimidyl 3-(trimethylstanny)benzoate. *Nucl Med Biol.* 2001;28:33–40.
12. Muthuswamy MS, Roberson PL, Buchsbaum DJ. A mouse bone marrow dosimetry model. *J Nucl Med.* 1998;39:1243–1247.
13. Berger MJ. *Improved Point Kernels for Electron and Beta Ray Dosimetry.* Washington, DC: National Bureau of Standards; 1973:73–107.
14. ICRU. *Stopping Powers and Ranges for Protons and Alpha Particles.* ICRU Report 49. Bethesda, MD: International Commission on Radiation Units and Measurements; 1993.
15. ICRU. *Methods and Assessment of Absorbed Dose in Clinical Use of Radionuclides.* ICRU Report 32. Washington, DC: International Commission on Radiation Units and Measurements; 1979.
16. Behr TM, Sgouros G, Stabin MG, et al. Studies on the red marrow dosimetry in radioimmunotherapy: an experimental investigation of factors influencing the radiation induced myelotoxicity in therapy with β^- , auger/conversion electron- or α -emitters. *Clin Cancer Res.* 1999;5:3031–3043.
17. Hamilton JG, Asling CW, Garrison WM, et al. The accumulation, metabolism, and biological effects of astatine in rats and monkeys. *Univ Calif Publicat Pharmacol.* 1952;2:283–344.